

# Diffusion-Weighted Imaging of Prostate Cancer

Ryota Shimofusa, MD,\* Hajime Fujimoto, MD,† Hajime Akamata, MD,† Ken Motoori, MD,\*  
Seiji Yamamoto, MD,\* Takuya Ueda, MD,\* and Hisao Ito, MD\*

**Objective:** The purpose of this study was to assess whether T2-weighted (T2W) imaging with diffusion-weighted (DW) imaging could improve prostate cancer detection as compared with T2W imaging alone.

**Methods:** The subjects consisted of 37 patients with prostate cancer and 23 without cancer undergoing magnetic resonance (MR) imaging. Using a 1.5-T superconducting magnet, all patients underwent T2W and DW imaging with parallel imaging. Images were independently reviewed by 3 readers to determine the detectability of prostate cancer. The detectability of T2W imaging without and with DW imaging was assessed by means of receiver operating characteristic analysis.

**Results:** Mean areas under the receiver operating characteristic curve for T2W imaging alone and for T2W imaging with DW imaging were 0.87 and 0.93, respectively. The receiver operating characteristic analysis showed that the addition of DW imaging to conventional T2W imaging significantly improved tumor detection ( $P = 0.0468$ ) compared with T2W imaging alone.

**Conclusions:** The addition of DW imaging to conventional T2W imaging provides better detection of prostate cancer.

**Key Words:** magnetic resonance imaging, prostate cancer, diffusion-weighted imaging, parallel imaging

(*J Comput Assist Tomogr* 2005;29:149–153)

The latest estimates of global cancer incidence show that prostate cancer is the third most common cancer in men, with half a million new cases each year.<sup>1</sup> In Japan, mortality attributable to prostate cancer is lower than in Western countries but is increasing rapidly.<sup>1,2</sup> Early detection of prostate cancer is vital for reducing mortality.

Recent reports have demonstrated the detectability of prostate cancer by magnetic resonance (MR) imaging.<sup>3,4</sup> On T2-weighted (T2W) imaging, regions of prostate cancer show decreased signal intensity relative to normal peripheral zone tissue because of increased cell density and a loss of prostatic ducts.<sup>4</sup> This finding is nonspecific, however, because other diseases such as prostatitis or hyperplasia can also cause low

signal intensity on T2W imaging.<sup>5–8</sup> Moreover, detection of prostate cancer in the transition zone, which is present in up to 30% of all prostate cancer, is difficult because this zone is the site of the origin of benign prostatic hyperplasia, which can have a heterogeneous appearance.<sup>9</sup>

Recently, diffusion-weighted (DW) imaging has been available for abdominal and pelvic lesions such as liver,<sup>10,11</sup> renal,<sup>12</sup> and ovarian tumors.<sup>13,14</sup> Some preliminary studies<sup>15–17</sup> have indicated that DW imaging can differentiate a malignant neoplasm from benign prostate tissue because of a significant difference in the apparent diffusion coefficient value. These studies did not evaluate the ability to detect human prostate cancer, however.

When obtaining DW images, susceptibility artifacts on echo planar imaging sequences often degrade the quality of images. This was the principal problem when obtaining DW images of the prostate, which is located adjacent to stool and gas in the rectum. With a recent technical evolution, a parallel imaging technique (sensitivity encoding [SENSE]) is now available, however. Using SENSE, less distorted DW images of human prostate are available, because susceptibility artifacts can be significantly reduced.<sup>18</sup> The purpose of this study was to determine the detectability of prostate cancer by T2W imaging with DW imaging as compared with T2W imaging alone.

## MATERIALS AND METHODS

### Patients

This was a retrospective study conducted at a single institution. Between February and November 2003, 124 consecutive patients with clinically suspected prostate cancer because of elevated ( $>4.0$  ng/mL) prostate specific antigen but with no prior treatment of prostate cancer underwent MR examination, including DW imaging. Sixty of the 124 patients had a histopathologic diagnosis proven by surgery or routine biopsy of 10 sites, including the central gland and peripheral zone. The other 64 patients were finally excluded from this study. Although a biopsy was planned for 30 of these 64 patients, it was not performed within the period of this study. The remaining 34 patients did not undergo biopsy at our institution because of 1) deterioration in general health ( $n = 12$ ), 2) multiple metastatic disease ( $n = 5$ ), 3) the patient's desire to be followed up without biopsy ( $n = 8$ ), and 4) the patient's desire to consult another hospital ( $n = 9$ ). The numbers of patients with surgically and biopsy-proven prostatic carcinoma were 18 and 19, respectively. Fourteen patients were free of malignancy on biopsy of 10 sites. Nine patients without cancer and undergoing transurethral resection because of symptoms of

Received for publication November 4, 2004; accepted January 6, 2005.

From the \*Department of Radiology, Chiba University Hospital, Chiba, Japan; and †Department of Radiology, Numazu City Hospital, Shizuoka, Japan.

Reprints: Ryota Shimofusa, Department of Radiology, Chiba University Hospital, 1-8-1, Inohana, Chuo-ku, Chiba City, Chiba, Japan, 260-8677 (e-mail: mofu@indigo.plala.or.jp).

Copyright © 2005 by Lippincott Williams & Wilkins

benign prostatic hyperplasia were also included. Overall, 37 (62%) of the 60 patients had prostate cancer. These patients underwent biopsy and/or surgery within 6 months after the MR examination. The mean patient age was 71 years (range: 54–82 years), and the mean prostate specific antigen value was 21.8 ng/mL (range: 4.5–130 ng/mL). Informed consent was obtained from all patients before MR imaging.

### Imaging Protocol

Magnetic resonance images were obtained with a 1.5-T MR imaging system (Gyrosan Intera; Philips Medical Systems, Best, The Netherlands). We used a 4-channel pelvic phased-array coil. All patients underwent DW imaging in addition to imaging using a routine prostatic MR protocol. This routine protocol included transverse, sagittal, and coronal T2W fast spin echo sequences (3800–4000 milliseconds/120 milliseconds repetition time/echo time, 20-cm × 20-cm field of view, 256–280 × 512 matrix, echo train length = 16, 3–4-mm slice thickness, 0.5-mm intersection gap, average of 2).

Axial DW images were obtained by the single-shot echo planar imaging technique using the following imaging parameters: 2500 milliseconds/90 milliseconds repetition time/echo time, 20-cm × 20-cm field of view, 128 × 128 matrix, 3–4-mm slice thickness, 0.5-mm intersection gap, average of 2. Isotropic DW images were obtained by using diffusion gradients with 2 b-values (0 and 1000 sec/mm<sup>2</sup>) along 3 directions of motion-probing gradients. We used a SENSE reduction factor of 2. The SENSE reduction factor is the ratio between the number of phase-encoding steps required for full-Fourier imaging and the number of phase-encoding steps necessary for an accelerated SENSE scan.

### Image Analysis

Images were interpreted by 3 readers (R.S., H.F., and H.A.) blinded to the results of biopsy or operation.

At first, T2W images alone were interpreted without knowledge of the results of DW imaging. The criterion for detecting prostatic cancer was a low-intensity mass relative to high-intensity background of the normal peripheral zone.<sup>4</sup> On the basis of the findings, the presence or absence of prostate cancer was estimated by the readers using a 5-point rating scale (definitely or almost definitely present = 5, probably present = 4, possibly present = 3, probably absent = 2, and definitely or almost definitely absent = 1). On T2W imaging, we also assessed the presence or absence of benign prostatic hyperplasia.

More than 2 weeks after the first reading, the 3 readers reviewed combined T2W and DW imaging. Because anatomic detail was unclear as the result of a low signal-to-noise ratio on DW images, we referred to axial T2W images of the same planes. We determined the diagnostic criteria of DW imaging as follows: focal hyperintense (relative to background prostatic structure) lesions almost definitely present received a score of 5, focal hyperintense lesions probably present received a score of 4, focal hyperintense lesions possibly present received a score of 3, focal hyperintense lesions probably absent received a score of 2, and focal hyperintense lesions almost definitely absent received a score of 1. These criteria were applied to all prostatic regions, including the central gland.

For the calculation of sensitivity and specificity, these results were dichotomized so that scores of 1 through 3 were rated as cancer absent and scores of 4 and 5 were rated as cancer present.

### Statistical Analysis

Receiver operating characteristic analysis was used to compare the results of routine T2W imaging alone and T2W imaging combined with DW imaging (rating scale range: 1–5). The area under the receiver operating characteristic curve (Az) was calculated for each reader and MR sequence. The statistical significance ( $P < 0.05$ ) of differences in the Az was determined by means of the unpaired Student *t* test. Receiver operating characteristic curves were estimated with the ROCKIT 0.9B beta version program (C. Metz, Chicago, IL). Sensitivity, specificity, positive predictive value, and negative predictive value were also calculated.

## RESULTS

The Az values, sensitivity, specificity, positive predictive value, and negative predictive value of the 3 readers are summarized in Table 1. All readers achieved higher sensitivity and specificity on combined T2W and DW imaging than on T2W imaging alone.

The Az values for the 3 readers for each T2W imaging and T2W imaging combined with DW imaging were 0.85 versus 0.93, 0.88 versus 0.96, and 0.87 versus 0.89, respectively. The mean Az value for each T2W imaging and combined T2W and DW imaging was 0.87 versus 0.93 (Fig. 1). Receiver operating characteristic analysis revealed that the addition of DW imaging to T2W imaging improved the diagnostic performance significantly ( $P = 0.0468$ ). There were no significant differences in diagnostic accuracy among the 3 readers ( $P > 0.05$ ).

Diffusion-weighted imaging clearly depicted prostate cancer as focal hyperintense areas (Figs. 2, 3). With the enhanced contrast between cancer and other prostatic tissue, T2W imaging with DW imaging resulted in a total 96 (86%) of

**TABLE 1.** Diagnostic Performance of T2W Imaging Alone and Combined T2W and DW Imaging for the Detection of Prostate Cancer

	Sensitivity (%)	Specificity (%)	Positive Predictive Value (%)	Negative Predictive Value (%)	Az
T2W imaging alone					
Reader 1	76	74	82	65	0.85
Reader 2	73	83	87	66	0.88
Reader 3	86	74	84	77	0.87
Mean	78	77	84	69	0.87
Combined T2W and DW imaging					
Reader 1	84	83	89	76	0.93
Reader 2	86	91	94	81	0.96
Reader 3	89	78	87	82	0.89
Mean	86	84	90	79	0.93

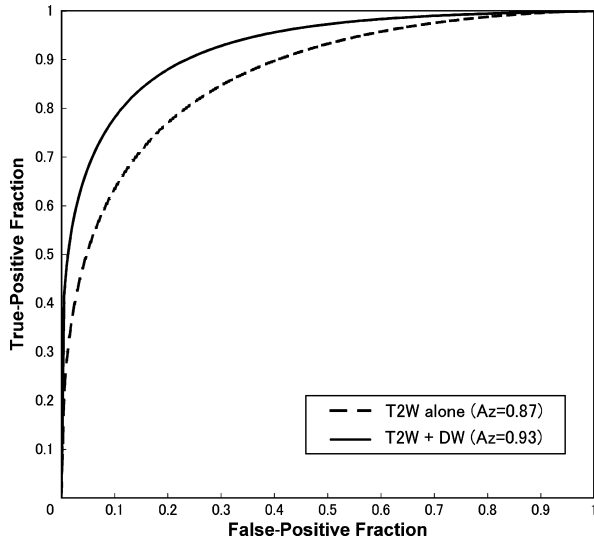


**FIGURE 1.** Mean receiver operating characteristic curves compare the performance of T2-weighted (T2W) imaging alone and combined T2W and diffusion-weighted (DW) imaging for detection of prostate cancer. The mean areas under the receiver operating characteristic curves (Az) of T2W imaging alone and combined T2W and DW imaging are 0.87 and 0.93, respectively. The difference between the 2 receiver operating characteristic curves is significant ( $P = 0.0468$ ).

111 (31 of 37 cases for reader 1, 32 of 37 cases for reader 2, and 33 of 37 cases for reader 3) reviewed cancerous cases being judged as positive, although with T2W imaging alone, 87 (78%) of the 111 (28 of 37 cases for reader 1, 27 of 37 cases for reader 2, and 32 of 37 cases for reader 3) reviewed cancerous cases were judged as positive. In addition, DW imaging might assist in detecting prostate cancer involving the transition zone, which is difficult to discriminate from other lesions such as benign prostatic hyperplasia on T2W imaging alone (see Fig. 3). Radical prostatectomy specimens demonstrated that 8 of 18 patients had cancer foci involving the transition zone. Diffusion-weighted imaging distinctly depicted the cancer in the transition zone as hyperintense (score 4 or 5 by all readers) in 5 (63%) of the 8 patients. On T2W

imaging alone, however, cancer in the transition zone could be clearly identified only in 1 (13%) of the 8 patients. This 1 patient had a cancer focus continuum involving the peripheral zone to the transition zone.

Diffusion-weighted imaging could differentiate between prostate cancer and some nonspecific hypointense lesions mimicking cancer on T2W imaging (Fig. 4). Of the total 180 (3 readers with 60 cases each) reviewed cases, there were 16 false-positive cases with T2W imaging alone, a number reduced to 11 cases with DW imaging. All readers also achieved a higher negative predictive value on combined T2W and DW imaging than on T2W imaging alone. Mean negative predictive values for T2W imaging alone and T2W with DW imaging were 69% and 79%, respectively.

### DISCUSSION

Magnetic resonance imaging is widely used for determination of prostatic disease. Because of the similarity in signal intensity between prostate cancer and other benign lesions such as benign prostatic hyperplasia on T2W imaging, however, conventional MR imaging has good sensitivity (78%–83%) but low specificity (50%–55%) in detecting and localizing prostate cancer.<sup>4–9</sup> Additional procedures, such as MR spectroscopy, have been applied to achieve a more specific diagnosis and localization of prostate cancer.<sup>19,20</sup> Combined MR imaging and spectroscopy indicated the presence of tumor with high sensitivity (95%) and high specificity (91%).<sup>20</sup> Magnetic resonance spectroscopy is not routinely used with commercially available MR systems, however. Some reports suggest that dynamic contrast-enhanced MR imaging can discriminate prostate cancer from normal prostatic tissue.<sup>21</sup> The reported sensitivity (74%) and specificity (81%) of the dynamic contrast-enhanced study for tumor detection are lower than those of MR spectroscopy, however, and are not significantly different from the values of conventional fast spin echo images.<sup>21</sup>

Diffusion-weighted imaging offers another solution for identifying cancer in the prostate. Because of the many tightly packed glandular elements with little central space for mucin or fluid storage in prostate cancer, apparent diffusion

**FIGURE 2.** Prostate cancer in a 63-year-old man. A, Axial T2-weighted fast spin echo image (4000 milliseconds/120 milliseconds repetition time/echo time) shows a 15-mm diameter hypointense tumor (arrow) in the left peripheral zone. B, Axial imaging-diffusion-weighted image of the same plane reveals a focal hyperintense tumor (arrow). A radical prostatectomy specimen revealed moderately differentiated adenocarcinoma.

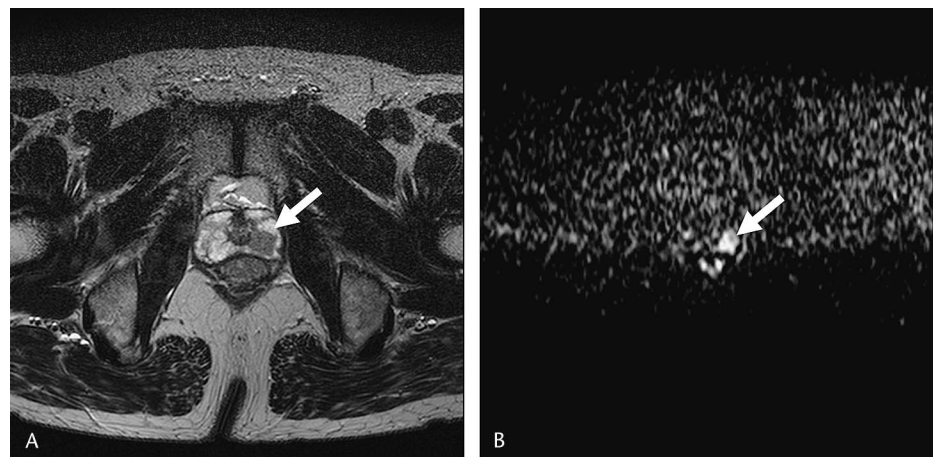
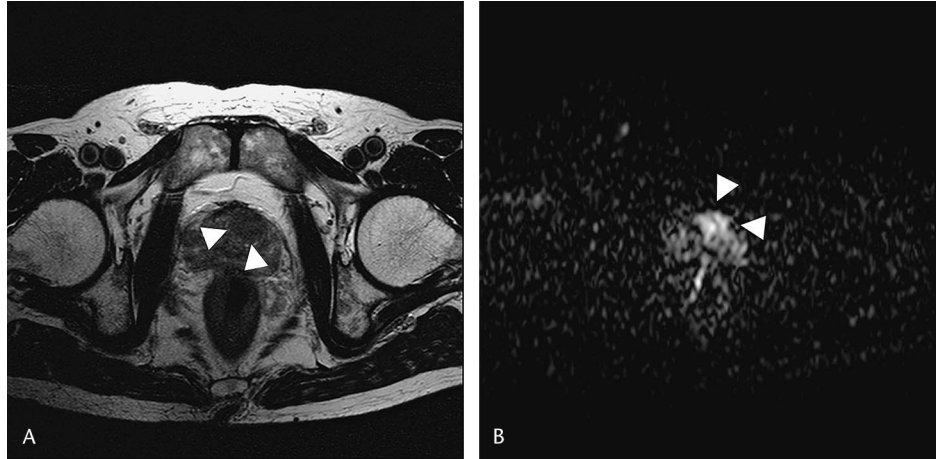


**FIGURE 3.** Prostate cancer in a 72-year-old man. A, Axial T2-weighted image (3880 milliseconds/120 milliseconds repetition time/echo time) shows a 20-mm diameter hypointense area in the left central gland (arrowheads). Discrimination of prostate cancer from other benign lesions, such as a benign prostatic hyperplastic nodule, is difficult. B, Axial imaging-diffusion-weighted image of the same plane clearly demonstrates a focal hyperintense lesion (arrowheads). A radical prostatectomy specimen revealed moderately differentiated adenocarcinoma.



coefficient values, which correspond to the restriction of water displacement, are reportedly significantly lower than in normal prostate.<sup>16</sup> Compared with MR spectroscopy, pelvic DW imaging is more easily performed on most MR scanners without additional software, although every system has several limitations. Without parallel imaging, however, DW imaging of the prostate is not performed as part of routine clinical MR imaging, mainly because of susceptibility artifacts that degrade the image and make it difficult to localize the tumor. Applying parallel imaging, the accumulating phase that causes susceptibility artifacts is decreased because of a reduction in the train of gradient echoes and sampling time. Shortened imaging times with parallel imaging also contribute to the suppression of motion artifacts.

To our knowledge, this is the first clinical study to apply DW imaging with parallel imaging and with a high b-value ( $b = 1000$ ) to the detection of prostate cancer. On DW imaging, prostate cancer was depicted as a hyperintense focal lesion with markedly enhanced contrast compared with T2W imaging (see Fig. 2). Therefore, we could differentiate cancers from noncancerous lesions with greater confidence. In addition, DW imaging has the capability of revealing prostate cancer not only in the peripheral zone but in the transition zone (see Fig. 3). The capability of detecting cancer in the transition zone gives

DW imaging a great advantage over conventional T2W imaging and MR spectroscopic imaging. The result of higher performance in the detection of prostate cancer was particularly related to this capability. Although there were differences in the patient populations, sensitivity (86%) and specificity (84%) on T2W imaging with DW imaging in our study without an endorectal coil were higher than those of former studies (sensitivity: 74%–83%, specificity: 50%–81%) with an endorectal coil<sup>4–9</sup> and a dynamic study.<sup>21</sup>

The apparent diffusion coefficient value was not quantified in the present study. Because we used a high b-value ( $b = 1000$ ) to enhance the contrast between normal and cancerous prostate, the signal-to-noise ratio was reduced and an adequate region of interest was not ensured in correlation with the pathologic specimen in the present study. This is usually the case for small lesions. Regardless of whether the precise apparent diffusion coefficient value is calculated or not, b-values of 400 to 500 as used in liver DW imaging<sup>10,11</sup> may be more appropriate for a balance between the signal-to-noise ratio and diffusion weighting. Even when using high b-values, it might be possible to improve the signal-to-noise ratio with increased averaging<sup>15</sup> and/or with the use of an endorectal coil modified for echo planar imaging by being inflated with liquid.<sup>17</sup> The most appropriate b-value for DW imaging of the prostate is

**FIGURE 4.** A 72-year-old man without prostate cancer. A, Axial T2-weighted image (3900 milliseconds/120 milliseconds repetition time/echo time) shows an enlarged prostatic gland as a result of benign prostatic hyperplasia. A small hypointense focus is detected in the left peripheral zone (arrow). Prostate cancer cannot be excluded on the basis of this appearance. B, Axial diffusion-weighted image of the same plane demonstrates no focal hyperintense lesion relative to other regions of the prostate. Biopsies of 10 sites, including the left peripheral zone, did not reveal a malignant focus.



still to be established. Further studies with various b-values, larger patient populations, and imaging sequence modifications are needed.

In conclusion, our results demonstrate the potential value of prostatic DW imaging in clinical practice. Diffusion-weighted imaging combined with T2W imaging provides a higher detection rate of prostate cancer.

## REFERENCES

1. Quinn M, Babb P. Patterns and trends in prostate cancer incidence, survival, prevalence and mortality. Part I: international comparisons. *BJU Int*. 2002;90:162–173.
2. Quinn M, Babb P. Patterns and trends in prostate cancer incidence, survival, prevalence and mortality. Part II: individual countries. *BJU Int*. 2002;90:174–184.
3. Thornbury JR, Ornstein DK, Choyke PL, et al. Prostate cancer: what is the future role for imaging? *AJR Am J Roentgenol*. 2001;176:17–22.
4. Yu KK, Hricak H. Imaging prostate cancer. *Radiol Clin N Am*. 2000;38:59–85.
5. Hricak H, White S, Vigneron D, et al. Carcinoma of the prostate gland: MR imaging with pelvic phased-array coils versus integrated endorectal-pelvic phased-array coils. *Radiology*. 1994;193:703–709.
6. Quint LE, Van Erp JS, Bland PH, et al. Prostate cancer: correlation of MR images with tissue optical density at pathologic examination. *Radiology*. 1991;179:837–842.
7. Lovett K, Rifkin MD, McCue PA, et al. MR imaging characteristics of noncancerous lesions of the prostate. *J Magn Reson Imaging*. 1992;2:35–39.
8. White S, Hricak H, Forstner R, et al. Prostate cancer: effect of postbiopsy hemorrhage on interpretation of MR images. *Radiology*. 1995;195:385–390.
9. Ikonen S, Kivisaari L, Tervahartiala P, et al. Prostatic MR imaging. Accuracy in differentiating cancer from other prostatic disorders. *Acta Radiol*. 2001;42:348–354.
10. Namimoto T, Yamashita Y, Sumi S, et al. Focal liver masses: characterization with diffusion-weighted echo-planar MR imaging. *Radiology*. 1997;204:739–744.
11. Ichikawa T, Haradome H, Hachiya J, et al. Diffusion-weighted MR imaging with a single-shot echoplanar sequence: detection and characterization of focal hepatic lesions. *AJR Am J Roentgenol*. 1998;170:397–402.
12. Squillaci E, Manenti G, Di Stefano F, et al. Diffusion-weighted MR imaging in the evaluation of renal tumours. *J Exp Clin Cancer Res*. 2004;23:39–45.
13. Moteki T, Ishizaka H. Diffusion-weighted EPI of cystic ovarian lesions: evaluation of cystic contents using apparent diffusion coefficients. *J Magn Reson Imaging*. 2000;12:1014–1019.
14. Katayama M, Masui T, Kobayashi S, et al. Diffusion-weighted echo planar imaging of ovarian tumors: is it useful to measure apparent diffusion coefficients? *J Comput Assist Tomogr*. 2002;26:250–256.
15. Gibbs P, Tozer DJ, Liney GP, et al. Comparison of quantitative T2 mapping and diffusion-weighted imaging in the normal and pathologic prostate. *Magn Reson Med*. 2001;46:1054–1058.
16. Song SK, Qu Z, Garabedian EM, et al. Improved magnetic resonance imaging detection of prostate cancer in a transgenic mouse model. *Cancer Res*. 2002;62:1555–1558.
17. Issa B. in vivo measurement of the apparent diffusion coefficient in normal and malignant prostatic tissues using echo-planar imaging. *J Magn Reson Imaging*. 2002;16:196–200.
18. Bammer R, Keeling SL, Augustin M, et al. Improved diffusion-weighted single-shot echo-planar imaging (EPI) in stroke using sensitivity encoding (SENSE). *Magn Reson Med*. 2001;46:548–554.
19. Kurhanewicz J, Vigneron DB, Hricak H, et al. Three-dimensional H-1 MR spectroscopic imaging of the in situ human prostate with high (0.24–0.7-cm<sup>3</sup>) spatial resolution. *Radiology*. 1996;198:795–805.
20. Scheidler J, Hricak H, Vigneron DB, et al. Prostate cancer: localization with three-dimensional proton MR spectroscopic imaging—clinicopathologic study. *Radiology*. 1999;213:473–480.
21. Jager GJ, Ruijter ET, van de Kaa CA, et al. Dynamic TurboFLASH subtraction technique for contrast-enhanced MR imaging of the prostate: correlation with histopathologic results. *Radiology*. 1997;203:645–652.